PCCP
Physical Chemistry Chemical Physics

Accepted Manuscript

This article can be cited before page numbers have been issued, to do this please use: F. Šebesta, M. T. H. Nguyen, M. Munzarova and J. V. Burda, *Phys. Chem. Chem. Phys.*, 2024, DOI: 10.1039/D4CP04386C.

ROYAL SOCIETY OF CHEMISTRY

rsc.li/pccp

On pH controlling of the reaction mechanism: Interactions of Au(I)-NHC Complex with Thioredoxin Reductase (modeled by Cysteine and Selenocysteine); ab initio and DFT calculations.

Filip Šebesta[a], Man Thi Hong Nguen [a], Markéta Munzarová[b], and Jaroslav V. Burda[a*]
[a]*Department of Chemical Physics and Optics, Faculty of Mathematics and Physics. Charles University, Ke Karlovu 3. 121 16 Prague 2, Czech Republic*
[b]*Department of Chemistry, Faculty of Natural Sciences, Masaryk University, Kamenice 5, 62500 Brno, Czech Republic*

corresponding author: jaroslav.burda@matfyz.cuni.cz

Abstract

Interactions of Cys and Sec amino acids with a simple model of Au(I)-NHC complex are explored using DFT functionals and post-HF methods. Besides the conventional quantum chemical description with NVT canonical ensemble, transformation to the grand-canonical ensemble is performed. In this way, chemical species with different number of protons can be considered and reactions at constant pH evaluated. For this purpose, a new thermodynamic state function is introduced with proton chemical potential as natural variable - Gibbs-Alberty free energy (ΔGA^0) and applied to Cys/Sec - Au(I)NHC interactions. Having determined all the necessary pK_a values, the pH dependent equilibrium constant can be expressed for both Cys and Sec coordination to the gold(I) complex. Dependences of ΔGA^0(Cys) and ΔGA^0(Sec) as functions of varying pH demonstrates visible preference for Sec coordination in acidic and neutral conditions, which is changed in the vicinity of pH ≈ 8 where Cys coordination becomes thermodynamically more stable.

Introduction

The thioredoxin system plays a key role in controlling the overall intracellular redox balance in cells. It is basically consisted of the small redox protein thioredoxin (Trx), nicotinamide adenine dinucleotide phosphate, in its reduced form (NADPH), and thioredoxin reductase (TrxR), a large homodimeric selenzoenzyme, which controls the redox state of thioredoxin. Its mechanism of action is clearly summarized in the study of Sun et al.[1] Crystalographic data and 3D structure of mammalian thioredoxin reductase was solved by Sandalova et al.[2,3] The active centers of the reductase is located in a small cavity close to the C-terminus of the enzyme. Details of a mechanism of selenoenzyme inhibition is still under investigation in several laboratories.[4,5] Nevertheless, the thioredoxin system is now clearly recognized as an effective

View Article Online
DOI: 10.1039/D4CP04386C

"druggable" target for the development of new anticancer drugs.[6,7,8] Accordingly, a number of established anticancer agents were retrospectively found to be potent inhibitors of thioredoxin reductases and to induce severe oxidative stress. Previously a variety of gold compounds, either gold(I) or gold(III), were reported to manifest outstanding antitumor properties forming a promising class of experimental anticancer agents.[9,10,11] In the study of Serratrice et al.,[12] it is noted that similar cytotoxic properties were observed in parent gold(III) complexes as in corresponding gold(I), which can lead to implication that gold(III) is possibly reduced to gold(I) in the cellular environment. On the other hand, the same laboratory discovered that there are gold(III) complexes that remain in oxidation state +3 in the adduct form with protein.[13] An extended set of small molecules, which can serve as inhibitors TrxR, were reported by Cai et al.[14] In their study besides Au, Pt, and Ru metallocomplexes, sulphur, selenium or tellurium containing compounds were examined, too.

As a biological target of the metallodrugs is supposed to be the above-mentioned small cavity close to the C-terminus in thioredoxin reductase. The active center can be effectively blocked by transition metal complexes. Namely, Au(I) complexes were found to have high affinity towards this site[5] and they have been recognized as a promising candidate for a new class of anticancer drugs already some time ago.[10] As one of the first compounds, Au(I) phosphine complexes were examined and it was demonstrated that they inhibit activities of both thioredoxin and thioredoxin reductase.[15] The inhibition was found to be more pronounced in breast cancer cells. Later, the same laboratory confirmed that also the Au(I) complex with N-heterocyclic carbene (NHC) ligands can serve as an anticancer drug attacking the mitochondrial enzymes.[16] In their study, several derivatives with methyl, i-propyl, n-butyl or t-butyl modifications of imidazole ring were explored. By tuning the ligand exchange reactions at the Au(I) center, authors designed lipophilic, and cationic Au(I) complexes that selectively induce apoptosis in cancer cells but not in normal cells and allow selective targeting of mitochondrial selenoproteins. Activity of Au(I) complexes with NHC ligands together with analogous Ag(I) complexes were compared with cisplatin finding similar antitumor IC_{50} parameters.[17]

Recently, Au(I) complexes with modified NHC were found more active against both colon and breast cancer cells in comparison with cisplatin or with auranofin.[18] Particularly, the dinuclear Au(I) phosphano-complexes have significantly lower IC_{50} for colorectal or breast cancer as reported by Sulaiman et al.[19] and Abogosh et al.[20] New thiolate gold(I) complexes, which inhibit the proliferation of different human cancer cells, were reported by Abas et al.[21] showing higher cytotoxic activity than cisplatin. Strong antiproliferative effects of Au(I)

View Article Online
DOI: 10.1039/D4CP04386C

complexes with NHC ligands were found also in another study exploring lung, colon, and breast tumors.[22]

A complementary computation QM/MM study on reduction of disulphide bridge of Trx structure (PDB ID 1EP7) was published by Rickard et al.[23] The interaction of an auranofin model with tetrapeptide sequence of TrxR was studied by DFT by Howell.[24] Higher gold activity to selenium site in comparison with sulphur of cysteine was confirmed. Lately, Delgado calculated Au^{3+}/Au^{+} standard reduction potentials of Au(III) complexes connected with anticancer treatment.[25] They came to the conclusion that the CAM-B3LYP functional in combination with the SMD solvation is superior to other examined computational models. Recently, DFT study on some other modified Au(I)-NHC complexes with ethylselenolate were published.[26]

In our study, we determined thermodynamic as well as kinetic parameters for the substitution reaction of a simple chloro(imidazol-2-ylidene)gold(I) model complex where Au(I)-NHC abbreviation will denote only this compound here after. Modeling its binding to TrxR, the substitution reaction on the Au(I)-NCH complex with cysteine (Cys) and selenocysteine (Sec) amino acids is explored combining various QM and DFT levels with D-PCM/sUAKS solvation single-point calculations. One of the most important parts of this study is devoted to determination of binding preference of the gold complex to selenium or sulphur site in the key sequence of TrxR in dependence on pH. The Sec and Cys amino acids can be regarded as a model of the active tetrapeptide redox center (Gly-Sec-Cys-Gly) in C-terminus of TrxR. Therefore, a new Legendre transformation of Gibbs free energy to grand-canonical ensemble regarding proton chemical potential has to be performed and, in this way, Gibbs-Alberty free energy evaluated to observe differences in complexation energies between gold and selenium or gold and sulphur in dependence on pH of the surrounding environment.

Computational Tools

All the explored molecules (amino acids, gold complexes, and supermolecular systems) are optimized using the DFT method. Two levels for determination of the reaction coordinate are chosen where the B3LYP functional[27,28,29,30] is combined with *a)* the double zeta quality basis set (6-31+G(d)) and Stuttgart-Dresden effective core potentials with corresponding pseudoorbitals -Opt/D level - or *b)* the triple-zeta basis set (6-311++G(2df,2pd)) and the same quality of pseudoorbitals (with 2fg-polarization and diffuse functions extension) – Opt/T level, as discussed in our previous papers.[31,32,33] The corresponding set of pseudoorbitals[34] for Au, S, Cl, and Se atoms are collected in the Supplementary material. The both optimization levels *a)*

View Article Online
DOI: 10.1039/D4CP04386C

and *b)* are supplied with the same COSMO solvation model[35] using UFF cavities and 1.10 scaling of the van der Waals atomic radii. At the same levels, a frequency analyses are performed to check a character of calculated stationary points on the potential energy surface (minima or transition states (TS)) of the explored molecular systems and to quantify nuclear degrees of freedom. In the final Gibbs free energy evaluation in the water solution, the entropy contributions of translational and rotational degrees of freedom are corrected as suggested by Wertz[36] and Goddard:[37]

$$S_{liq}^{trans+rot} = \left(S_{gas}^{trans} + S_{gas}^{rot} - 14.3\right)\cdot 0.54 + 8.0 \qquad \text{(eq 1)}.$$

These corrections originate from the fact that translational and rotational degrees of freedom are visibly reduced in liquid phase in comparison with gas phase. For closer insight cf. Supplementary Information - part 2 (SI). In this way, the first estimation of the searched reaction Gibbs free energy profiles is determined. The higher optimization model Opt/T is used since it is computationally affordable for these small molecules and should provide more accurate results. Later, knowledge of differences between models Opt/D and Opt/T can be utilized for error estimation for more extended systems when no other choice (then Opt/D model) is possible, which is expected in our next studies on this topic. We are working on QM study using tetrapeptide as well as QM/MM approach for the complete TrxR monomeric unit interacting with this Au(I)-NHC model complex. In order to compare accuracy of the optimization processes, the geometries (selected bond lengths), AIM (bond) critical points, and energetical relations are compared.

Determination of reaction thermodynamic and kinetic parameters is performed at several computational levels for stationary points optimized at both Opt/D and Opt/T levels using more accurate single-point calculations (SP). They differ in basis sets, employed implicit solvation models or evaluation of electronic structures using besides DFT also post-HF methods.

I) DP-models (SP with D-PCM): Since the pH-dependent thermodynamic model has to be used (cf. below), the first choice relates to a recently developed model for reliable determination of pK_a values of amino acids, peptides, and proteins. SP energies are evaluated at the DFT/6-311++G(2df,2pd)/D-PCM/scaled-UAKS computational level[38,39] as described in our previous papers[40,41,42]. Two functionals are employed – B3LYP because of continuity and M06-2X, which provides better agreement between calculated and experimental pK_a values.[43] These functionals are further complemented with Grimme's D3 empirical dispersion and also with Becke-Johnson (BJ) dumping functions for the B3LYP functional. The D-PCM solvation

View Article Online
DOI: 10.1039/D4CP04386C

model with scaled-UAKS cavities was found recently as one of the best options for simulation of the water solution for pK_a evaluations.[43] The cavity rescaling is performed based on the actual NBO charges[44,45] and the original UAKS cavities as suggested by Tomasi,[46] Barone,[47] and extended by Orozco and Luque.[48,49] Atomic radii R_X are linearly scaled using partial charge ($q^{NBO}_{X,actual}$) of the actual atomic groups X (thiol, chloride, carboxyl oxygens) in an examined molecule relative to the change of its partial charge ($q^{NBO}_{X,prot}$ - $q^{NBO}_{X,dep}$) in reference molecules with protonated and deprotonated group X.[40,34,41,42,50] This can be expressed by formula:

$$R_X = R^0_X + \gamma \cdot \frac{q^{NBO}_{X,actual} - q^{NBO}_{X,dep}}{q^{NBO}_{X,prot} - q^{NBO}_{X,dep}} \qquad \text{(eq 2)}$$

where the scaling factors γ and the radii R_X^0 from the original UAKS model are utilized.[48,49] Using partial charges instead of formal ones leads to smooth and more consistent results. The reference molecules chosen for determination of partial charges on the given groups X in the deprotonated $q^{NBO}_{X,dep}$ and protonated form $q^{NBO}_{X,prot}$ are taken as suggested in the original UAKS approach.[48] Besides electrostatic solvation energy, non-electrostatic (repulsion, dispersion, cavitation) terms are also included in the total Gibbs free energy of the explored system. This model is applied for both optimal geometries obtained at the Opt/D and Opt/T level and labeled as DP/D (DP_B3/D and DP_M06/D) and DP/T (only for B3LYP) here after, respectively.

IIa) CP/T model (SP with C-PCM): For a comparison, geometries from double-zeta optimization Opt/D are further employed in the same SP calculations B3LYP-GD3BJ/6-311++G(2df,2pd) using COSMO solvation model together with Klamt cavities.

IIb) CP/Q model: In analogy with extension from DP/D to CP/T, the B3LYP-GD3BJ computational level is considered for model Opt/T where energy profiles are determined in combination with quadruple-zeta basis set aug-cc-pVQZ for H, C, N, O atoms,[51,52] S and Cl atoms[53] and consistently with aug-cc-pVQZ-PP for Se[54] and Au[55,56] atoms taken from Basis Set Exchange.[57,58,59] This computational level is also supplemented with the COSMO/Klamt solvation model.

In order to demonstrate the accuracy of the previous computational levels, the last pair of computational models is evaluated based on CCSD(T) calculations for the structures obtained only using the Opt/T optimization model.

IIIa) MP2/D and CC/D model: The reaction profile is evaluated at CCSD(T)/6-31+G(d))/D-PCM/scaled-UAKS level of theory.

IIIb) MP2/T, CC/T, and CC/Te models: The CCSD(T)/6-311++G(2df,2pd)/D-PCM/scaled-UAKS level (signed as CC/T) is determined only for the deprotonated branch of the reaction scheme. Since these calculations are extremely CPU-demanded the protonated species are

evaluated only using the MP2/6-311++G(2df,2pd) computational level for the safe of computational time and the higher level of correlation contributions are estimated based on the formula:[60,61]

$$\Delta E_{CCSD(T)/TZP} = \Delta E_{MP2/TZP} + \left[\Delta E_{CCSD(T)/DZP} - \Delta E_{MP2/DZP}\right], \text{(eq 3)}$$

conserving in some sense correlation effects from lower-basis set to higher basis set calculations. In all the CCSD(T) calculation, the D-PCM/scaled-UAKS solvation model is used (labeled as CC/Te).

All the above-mentioned SP calculations are also complemented with Wertz's corrections of liquid environment from the corresponding level of optimization. Electronic properties of the process are further investigated using NBO and QTAIM for geometries using the optimization model Opt/D.

All the necessary pK_a values are determined at the DP/D level (both M06-2X and B3LYP) and compared also with values obtained at the DP/T and post Hartree-Fock levels according to the formula:

$$pK_a = \Delta G^0/(2.303RT) \qquad \text{(eq 4)}$$

considering reaction Gibbs free energy ΔG^0 for the deprotonation reaction:

$$HA + H_2O \rightarrow H_3O^+ + A^- . \qquad \text{(eq 5)}$$

R and *T* represent Avogadro constant and temperature at which the deprotonation occurs. In addition, the correction term $-\log[H_2O] = -1.74$ for the standard state of bulk water is used. For a deeper insight to this problematics cf. ref. 62.

Results and Discussion

Protonation states of reactants and products – pK_a evaluations

Modeling the substitution reaction where the chloro ligand of Au(I)-NHC complex is replaced by Cys or Sec amino acids (cf. **Scheme 1**) is investigated for different protonation states of reactants and products in correspondence to different pH. This means consideration of several protonated forms of acidic and basic functional groups, namely, carboxyl, thiol/selenol, and amino groups in Cys/Sec, the imidazole group in Au(I)-NHC complex, and their adducts. For each protonation state, several local minima are compared to identify the global minimum at both Opt/D and Opt/T optimization levels. This step is crucial to get correct pK_a values and energy differences between stationary points on energy profiles.

View Article Online
DOI: 10.1039/D4CP04386C

It is generally known (e.g. ref.[43] and citations within that paper) that most of the directly applied PCM models are not able to match the experimental pK_a values with sufficient accuracy.[63,64,65] Hence, in our previous series of papers, we suggested a general strategy how to determine pK_a usually within one log unit, which is based on the D-PCM model with scaled UAKS cavities and corresponds to the DP models in this study.[40-42, 50] In this way, SP energy evaluations are conducted with both B3LYP (DP_B3/D model) and M06-2X functionals (DP_M06/D) for geometries obtained at the Opt/D level and for structures optimized at the Opt/T level, only the B3LYP functional (DP/T) is used. The pK_a values are calculated according to (eq 4) and are summarized in **Table 1** for the relevant (de)protonated states of both isolated reactants and products. It can be noticed that especially DP_M06/D values are reasonably close to measured data[66,67] (RMSD difference ca 2.2 log unit). Overestimated pK_a values are particularly obtained for the most basic values (deprotonation of amino groups). For such negative ionic states (-2e), simple linear cavity-scaling is probably already not appropriate. The pK_a evaluation with more extended basis sets usually leads to lower accuracy since the UAKS model is optimized for DFT method with double-zeta basis set as other advanced solvent models. Similarly, higher level of theory (post Hartree-Fock methods) does not lead to more accurate pK_a predictions and similarly also the larger basis set further deteriorates the results, for deeper insight cf. ref [43]. Basically, the main reason is related to the fact that all cavity parameters were fitted to DFT double-zeta methods. It should be stressed that K_a are exponentially dependent on free energies. Therefore, even a small change makes visible difference in value of equilibrium constant.

Besides amino acid functional groups, pK_a of N-coordinated hydrogen atoms of Au(I)-NHC complex are also explored for the sake of completeness. Nevertheless, it is confirmed that Au(I)-NHC hydrogens (better naming than protons) have pK_a values in very high basic range, definitely above 14, as follows from **Table 1**. Such a high value also corresponds with the fact that in experimentally used complexes, these hydrogens are replaced by some bulky organic ligands, which are not cleaved within coordination of the Au(I)-NHC complex to the active site in the vicinity of TrxR C-terminus.

Energetics of the Interaction of Au(I)-NHC complex with Cys and Sec amino acids

Initially, the substitution reactions will be investigated supposing standard canonical ensemble. Owing to experimental pK_a values of 8.3 for thiol in Cys and 5.7 for selenol in Sec, both protonation states of mentioned groups are considered and, in this manner, deprotonated and

View Article Online
DOI: 10.1039/D4CP04386C

protonated branches are introduced in calculations where the reactants contain thiol or selenol and thiolate or selenolate anion, respectively. In product complexes of the protonated branch, no proton is bound to the S or Se atom. This proton is moved to the nearest oxygen of amino acid as follows from the calculated pK_as (**Tab. 1**). So that both the carboxyl and amino groups are protonated (NH_3^+). In total, we have two reaction branches for each amino acid which can further differ in their reaction mechanism.

Having optimized the isolated species (all necessary forms of Cys and Sec as well as the Au(I)-NHC complex), several different H-bonded associates of Cys/Sec amino acid with the Au(I) complex are searched for optimal reactant supermolecules as a starting point for determination of activation barriers. Similarly in products, stable supermolecular forms where structures with Au-S/Au-Se coordination are associated with the released chloride particle are examined (cf. **Scheme 1**). A reaction energy profile is completed with determination of transition state (TS) structures. In the case of the deprotonated branch, a single-step reaction mechanism exists with the TS structure characterized by one negative vibration mode corresponding to an antisymmetric stretch of Au-Cl and Au-S(Se) bonds. When the thiol (-SH) and selenol (-SeH) groups are present in the protonated branch, two different mechanisms can be distinguished. Either a two-step reaction mechanism where proton is first transferred from the S/Se site to one of the electronegative oxygen atoms of the carboxyl group and subsequently metallo-complex coordinates to S/Se atom or a single-step mechanism where both processes occur simultaneously.

All the various SP methods described in *Computational Tools* are applied for determination of reaction energy profiles and obtained activation and reaction free energies are collected in **Table 2**. Although the energies determined for dissociation constants at the CC/T level are not the best in comparison with experimental data (cf. **Table 1**), it is still assumed that the Gibbs free reaction energies evaluated at this level represents the most accurate approximation. However, these calculations are extremely demanding. Therefore, such calculations are only performed in the deprotonated branch, which contains a smaller set of molecules. For all protonated systems, the corresponding energies are estimated based on (eq 3) where relatively modest calculations at the MP2/TZP level are supplemented by energy corrections beyond second order of the perturbation theory, i.e. differences between CCSD(T) and MP2 values received at the cheaper CCSD(T)/DZP level, as used frequently before.[31, 32, 60, 61, 68] Quality of these estimations can be assessed from comparison of reaction and activation energies in the deprotonated branch. Since the estimation is relatively plausible with the maximal difference lower than 0.3 kcal/mol (cf. Table 2 last two columns), the estimated Gibbs

View Article Online
DOI: 10.1039/D4CP04386C

free energies will be considered as a reference for both reaction branches for the sake of consistency.

The determined reaction energy profiles (cf. **Fig. 1)** show that both reaction branches preferentially pass through a single activation barrier. Their heights are in all explored computational models higher in Cys involving reactions than in Sec one despite small energy differences in the case of deprotonated TS structures obtained at computational levels utilizing double zeta basis set (xxx/D models in **Table 2**) where the differences are often below 1 kcal/mol. Considering the two-step reaction mechanism within the protonated branch, the first activation barrier (TS1) corresponding to proton transfer to the carboxyl oxygen is usually lower in energy than the second activation barrier (TS2), which is connected with replacement of chloro-ligand by formation of coordination bond between the S/Se site and Au(I). It can be concluded that TS energies at least of the second barrier are visibly higher in complexes with Cys than Sec, cf. **Table 2**. Nevertheless, as mentioned above the single-step reaction mechanism is associated with visibly lower activation barriers. Another important conclusion of this part follows from comparison of TS energies of deprotonated and protonated branches. Namely, activation barriers in protonated branches are usually predicted lower than barriers connected with deprotonated forms. In comparison with study of Tolbatov et al.[26] their activation barriers are in good accord with our results, nevertheless, their reaction energies are, on the contrary to our calculations, endoergic since they have used for interaction of ethylselenolate with quite different gold(I) complex connected with more complex reaction mechanism.

Focusing on the reaction Gibbs free energies, the reactions with Sec are generally slightly more exergonic than with Cys. This higher exoergicity is more clearly seen in the case of protonated systems where the difference is generally more than 3 kcal/mol. Substantially smaller energy difference can be observed for deprotonated amino acids where usually the exoergicity difference is less than 1 kcal/mol. It is also worth to notice that the deprotonated reaction branches exhibit a visibly higher exergonic character in comparison with the protonated branches, which is associated with protonation of the carboxyl oxygen in the course of the substitution reaction.

Kinetic aspects

Applying Eyring's transition state theory on reaction energy profiles determined in previous section, estimation of reaction rates can be obtained. In the case of the single-step mechanism

View Article Online
DOI: 10.1039/D4CP04386C

where the system needs to pass only over one TS, it leads to a simple estimation of rate constants according to $k = \frac{k_B T}{h} e^{\left(-\Delta G^{\ddagger}/RT\right)}$ formula where $\Delta G^{\ddagger}$ corresponds to the Gibbs free activation barrier, k_B, R, and h are Boltzmann, universal gas, and Planck constants, respectively, and all rate constants are determined at the temperature T = 298 K. For the two-step mechanism with rate constants k_1, k_2 for forward steps and k_{-1} and k_{-2} for the pertinent reverse reactions, the total rate constant can be derived based on steady-state intermediate I, i.e. $d[I]/dt \approx 0$ and supposing $k_1 \ll k_{-1}$, $k_2 \gg k_{-2}$, which leads to the total rate constant[69] (cf. SI part 3):

$$k_{tot} = \frac{k_1.k_2}{k_{-1}+k_2}. \qquad \text{(eq 6)}$$

Results for the deprotonated branch are collected in the upper part of **Table 3** and total k_{tot} together with partial rate constants k_1, k_{-1}, k_2, k_{-2} for the protonated branch in the lower part. They show that all the computational levels predict faster reaction rate for Sec than for Cys in the case of the single-step mechanism in both branches with the only CP/T exception for the protonated branch. Based on the total rate constants, the same conclusion is also valid for the two-step mechanism where it can be seen that the conditions for steady state intermediate are fulfilled, and estimation of the total rate constant is sufficiently justified. The total rate constants also confirm significant preference (faster occurrence) for the one-step in comparison with two-step reaction mechanism as it ensues from the activation barriers. An important finding is that the substitution reactions for amino acids with the protonated S/Se site are visibly faster than in the case of deprotonated ones. This means that the reaction course will be faster in acidic solutions than in basic environment. Nevertheless, according to the relatively large values of all the rate constants, it is evident that the reaction rate is still quite fast from human perspective (using millimolar concentrations, it should be still finished on a sub-second scale).

Transformation to grand-canonical ensemble

Up to now we regarded the explored reaction in the framework of standard canonical ensemble. Nevertheless, when biochemical or biophysical processes are studied often constant pH environment must be considered. In order to cope with such conditions, Legendre transformation of Gibbs free energy to the grand-canonical description is required. In this manner, a new thermodynamic state function, Gibbs-Alberty free energy (GA), is introduced:[70,71,72,73]

$$dGA = dG - d(n(H^+).\mu(H^+)) = -SdT + VdP + \sum_{i\neq H^+} \mu_i.dn_i - \sum_{i=H^+} n_i.d\mu_i, \quad \text{(eq 7)}$$

View Article Online
DOI: 10.1039/D4CP04386C

where the first sum concerns basically all non-polar molecules while the second summation deals with polar or ionic species, which can differ by number of active protons. On the contrary to Gibbs energy where pressure, temperature, and molar 'concentrations' are intrinsic variable, the introduced new thermodynamical potential (Gibbs-Alberty free energy) is function of pressure, temperature, and chemical potentials – in our case proton chemical potentials as defined e.g., in ref.[41,42,50,74,75] In this way reactions cannot run to the standard chemical equilibrium, i.e. till the concentration of individual species are constant ($dn_i = 0$) but till the changes in chemical potential are zeroed ($d\mu_i = 0$). In our case, this means proton chemical potentials of individual species active in the explored chemical reaction where the exchange of protons is important. Actually, change of protonation state is the controlling element for varying pH of solution. An illustrative case is the proton chemical potential of water, which is defined as:

$$\mu^{PCP}(H_2O) = RT.ln\left(\frac{K_a^{[OH^-]}}{[H^+]} + 1 + \frac{[H^+]}{K_a^{[H_3O^+]}}\right). \text{ (eq 8)}$$

In analogous way proton chemical potential of all species from **Scheme 1** have to be evaluated and combined to grand-canonical equilibrium constant:

$$K' = \frac{[Au{-}NHC{-}Cys(COO)^+].[Cl^-]}{[Au{-}NHC].[Cys(COO)]}.f(pH) \text{ (eq 9)}$$

where $f(pH)$ is defined from the corresponding proton chemical potentials:

$$\text{f(pH)} = \frac{\left\{1+ \frac{[\text{H}^+]}{\text{K}_\text{a}^{[\text{HCl}]}}\right\}}{\left\{1+ \frac{\text{K}_\text{a}^{[\text{Au(NHC)}]}}{[\text{H}^+]}\right\}} * \frac{\left\{ \frac{[H^+]^2}{K_a^{[\text{Au-NHC-Cys(S)}]}.K_a^{[\text{Au-NHC-Cys(COO)}]}} + \frac{[H^+]}{K_a^{[\text{Au-NHC-Cys(COO)}]}} + 1 + \frac{K_a^{[\text{Au-NHC-Cys(N}H_2)]}}{[H^+]} + \frac{K_a^{[\text{Au-NHC-Cys(N}H_2)]}.K_a^{[\text{Au-}(NHC)^-\text{-Cys(}NH_2)]}}{[H^+]^2} \right\}}{\left\{\frac{[\text{H}^+]}{\text{K}_\text{a}^{[\text{Cys(COO)}]}} + 1 + \frac{\text{K}_\text{a}^{[\text{Cys(S)}]}}{[\text{H}^+]} + \frac{\text{K}_\text{a}^{[\text{Cys(S)}]}\text{K}_\text{a}^{[\text{Cys(N}H_2)]}}{[\text{H}^+]^2}\right\}}$$

(eq 10).

As mentioned already above the ΔGA^0 is function of chemical potential. It means when the pH dependence of reaction energy is search, this new grand-canonical thermodynamic potential is the only possibility (under constant p and T) how to evaluate it. One basic shortcoming is the fact that all the required pK_a have to know. Nevertheless, when only short pH range is explored the expression in eq 10 can be drastically reduced. For example, for energy determination in pH = (6-8) the following reduction can be obtained:

$$\text{f(pH)} = \frac{\left\{1 + \frac{K_a^{[\text{Au-NHC-Cys(N}H_2)]}}{[H^+]}\right\}}{\left\{1+ \frac{\text{K}_\text{a}^{[\text{Cys(S)}]}}{[\text{H}^+]}\right\}} \text{ (eq 10 reduced)}$$

since all the other forms differing in protonation state will contribute only very marginally.

View Article Online
DOI: 10.1039/D4CP04386C

Labeling of individual deprotonation states is given in **Table 1**. If different protonated forms of some reactant or product are used in the first part of K' then the f(pH) part has to be modified correspondingly e.g., proton chemical potential of that concrete form must be used. So that when water would be part of the reaction and we decide to use [OH^-] instead then its proton chemical potential must be considered, too and the f(pH) function modified correspondingly:

$$\mu^{PCP}(OH^-) = RT.ln\left(1 + \frac{[H^+]}{K_a^{[OH^-]}} + \frac{[H^+]^2}{K_a^{[OH^-]}.K_a^{[H_3O^+]}}\right) \quad \text{(eq 11)}$$

or in our case regarding fully protonated form of Cys(COOH), the second term in denominator will be based on following proton chemical potential:

$$\mu^{PCP}(Cys(COOH)) = RT.ln\left(1 + \frac{K_a^{[Cys(COO)]}}{[H^+]} + \frac{K_a^{[Cys(COO)]}K_a^{[Cys(S)]}}{[H^+]^2} + \frac{K_a^{[Cys(COO)]}K_a^{[Cys(S)]}K_a^{[Cys(NH_2)]}}{[H^+]^3}\right). \text{(eq 12)}$$

The value of K' is fully independent on the choice of particular forms of reactant or product considered in the evaluation of (eq 10) supposing that all the reaction energies and pK_a calculations are performed at the same computational level. Finally, it should be mentioned that species, which have pK_a negative or too large (say over 14), can be omitted from (eq 9) since their contribution is negligibly small if the explored pH range is e.g., between 2 and 12. In our case, it is for instance the term $\frac{[H^+]}{K_a^{[HCl]}}$ since pK_a(HCl)≈ -10.1 (at the M06-2X level) or $\frac{K_a^{[Au(NHC)]}}{[H^+]}$ with pK_a(Au(I)-NHC)= 16.1 log unit. Finally, pH dependent Gibbs-Alberty free reaction energy (ΔGA^0) is obtained from equilibrium constant K' based on van't Hoff reaction isotherm:

$$\Delta GA^0 = -RT.\ln(K') \quad \text{(eq 13)}.$$

For detailed analysis of ΔGA^0 it is worth to focus on the behavior of proton chemical potentials of individual species. For future insight into ΔGA^0 free energy as a function of pH, it is useful to inspect plots of proton chemical potential of neutral molecules Cys, and Sec in dependence on pH for both isolated amino acids and coordinated to Au(I)-NHC complex, which are presented in **Fig. 2** for the M06-2X/6-31+G(d)/D-PCM/sUAKS computational model.

Applying the above-mentioned to the grand-canonical model together with all the necessary pK_a values, pH dependent equilibrium constant K' can be determined according to (eq 9) and (eq 10). Consequently, the Gibbs-Alberty free reaction energy (ΔGA^0) in dependence on pH is received from (eq 13) for both reactions with Cys and Sec, which are plotted in **Fig. 3**.From the detailed inspection of **Fig. 2**, it can be noticed that all the changes in the slopes of both curves in **Fig. 3** are associated with changes of protonation states of the given reactant or product molecules depicted in **Fig. 2**. The other reactant (Au(I)-NHC) or product (Cl^-) species

View Article Online
DOI: 10.1039/D4CP04386C

do not contribute to any slope change since their pK_a are out of the explored range (cf. discussion in previous paragraph)

Regarding the presence of these two amino acids in the reduction center on C-terminus of TrxR (…Ser-Gly-Cys-Sec-Gly), preference for gold(I) coordination to one or the other amino acid is important for deeper understanding of a possible reaction mechanism of metal coordination to this active site and blocking natural enzyme functioning. From the plot in **Fig. 3**, it can be seen that for pH lower than 8 a preferential coordination to the Se site of Sec occurs while in more basic solutions the S site of Cys is used for coordination. However, if this has some tangible consequences in real behavior of the enzyme must be proven by some additional *in vitro* or *in vivo* experimental study focusing on this particular fact.

Conclusions

In this contribution, substitution reactions of model Au(I)-NHC complex with Cys and/or Sec amino acid are studied. The B3LYP and M06-2X functionals are used together with the post-HF (MP2 and CCSD(T)) methods combined with double- to quadruple-zeta basis sets. These computational levels are complemented with the D-PCM/sUAKS or C-PCM/Klamt implicit solvation model for determination of pK_a values and reaction energy profiles. The explored reaction is predicted exoergic for both protonated and deprotonated S/Se site within all applied computational models. Nevertheless, the deprotonated branch gives more pronounced energy release (is more exergonic) in comparison with the protonated branch. Also, energetic preference for Sec in the framework of canonical ensemble is noticeable and visibly more distinguished in the protonated branch. Regarding activation barriers, higher energies of transition states in Cys reactions are obtained in majority of the computational approaches in the single-step (preferable) reaction mechanism for both protonated and deprotonated branches, with a more visible differences in the deprotonated branch. These conclusions are also reflected in rate constant magnitudes estimated from Eyring's transition state theory where a relatively fast course of the substitutions can be expected. For the deprotonated branch, the reaction course is predicted for micromolar concentrations still within sub-second timescale.

In the second part of the study, Legendre transformation from the canonical to grand-canonical ensemble is performed leading to equilibrium constants *K'* dependent on acidity of solution. Such calculations require pK_a's evaluations of functional groups in the vicinity of pH range of interest. In accord with our previous study, these values for known systems (Cys, Sec, HCl, and water) were reproduced with reasonable accuracy at the M06-2X/6-31+G(d)/D-PCM/sUAKS level even in comparison with post-HF methods (MP2 and CCSD(T)). From the

transformed equilibrium constants *K'*, the Gibbs-Alberty free energies are subsequently evaluated for Cys and Sec interaction with Au(I) complex in dependence on solution pH. By comparing the course of both Cys and Sec energy curves, there is evident preference of Sec coordination to the gold complex in acidic and neutral solutions while in basic environment (with pH > 8) formation of Au-(S-Cys) is more exergonic. This result should be considered from perspective of the TrxR enzyme where both amino acids are in tight neighborhood. From this point, different coordination site can be controlled by changing pH in the cellular environment.

Concerning the introduced new thermodynamic potential, it has to stated that, when chemical process will be studied where for each reactant and product only single form (considering protonation) exist e.g., water at pH=7 and remaining concentrations of other protonation states (OH^- and H_3O^+) could be neglected then both standard way using canonical and this new one applying grand-canonical formulas approaches will give the same results ($\Delta GA^0 = \Delta G^0$). However, when more than one protonated form will be present in system (e.g., cysteine at pH=8.3 will have equal number of protonated and deprotonated forms of the thio-group) then no other option than grand-canonical approach should not be used. The only disadvantage is that all the required pK_a have to be known.

Acknowledgement

The authors are grateful to the Grant Agency of Czech Republic No 23-06909S for support of this project. We also highly appreciate generous admission to computing facilities owned by parties and projects contributing to the National Grid Infrastructure MetaCentrum, provided under the program "Projects of Large Infrastructure for Research, Development, and Innovations" (LM2010005).

References

(1) Sun, Q.-A.; Kirnarsky, L.; Sherman, S.; Gladyshev, V. N. Selenoprotein oxidoreductase with specificity for thioredoxin and glutathione systems. *PNAS* **2001**, *98*, 3673–3678. DOI: www.pnas.orgycgiydoiy10.1073ypnas.051454398.
(2) Sandalova, T.; Zhong, L.; Lindqvist, Y.; Holmgren, A.; Schneider, G. Three-dimensional structure of a mammalian thioredoxin reductase: Implications for mechanism and evolution of a selenocysteine-dependent enzyme. *PNAS* **2001**, *98*, 9533–9538.
(3) Cheng, Q.; Sandalova, T.; Lindqvist, Y.; Arnér, E. S. Crystal structure and catalysis of the selenoprotein thioredoxin reductase 1. *J. Biol. Chem.* **2009**, *284*, 3998-4008.

(4) Bindoli, A.; Rigobello, M. P.; Scutari, G.; Gabbiani, C.; Casini, A.; Messori, L. Thioredoxin reductase: A target for gold compounds acting as potential anticancer drugs. *Coordination Chemistry Reviews* **2009**, *253* (11-12), 1692-1707. DOI: 10.1016/j.ccr.2009.02.026.
(5) Rackham, O.; Nichols, S. N.; Leedman, P. J.; Berners-Price, S. N.; Filipovska, A. A gold(I) phosphine complex selectively induces apoptosis in breast cancer cells: Implications for anticancer therapeutics targeted to mitochondria. *Biochem. Pharmacol.* **2007**, *74*, 992–1002.
(6) Coronnello, M.; Mini, E.; Caciagli, B.; Cinellu, M. A.; Bindoli, A.; Gabbiani, C.; Messori, L. Mechanisms of cytotoxicity of selected organogold(III) compounds. *Journal of Medicinal Chemistry* **2005**, *48* (21), 6761-6765. DOI: 10.1021/jm050493o.
(7) Gabbiani, C.; Mastrobuoni, G.; Sorrentino, F.; Dani, B.; Rigobello, M. P.; Bindoli, A.; Cinellu, M. A.; Pieraccini, G.; Messori, L.; Casini, A. Thioredoxin reductase, an emerging target for anticancer metallodrugs. Enzyme inhibition by cytotoxic gold(III) compounds studied with combined mass spectrometry and biochemical assays. *Medchemcomm* **2011**, *2* (1), 50-54. DOI: 10.1039/c0md00181c.
(8) McKeage, M. J. Gold opens mitochondrial pathways to apoptosis. *British Journal of Pharmacology* **2002**, *136* (8), 1081-1082. DOI: 10.1038/sj.bjp.0704822.
(9) Urig, S.; Fritz-Wolf, K.; Reau, R.; Herold-Mende, C.; Toth, K.; Davioud-Charvet, E.; Becker, K. Undressing of phosphine gold(I) complexes as irreversible inhibitors of human disulfide reductases. *Angewandte Chemie-International Edition* **2006**, *45* (12), 1881-1886. DOI: 10.1002/anie.200502756.
(10) Rigobello, M. P.; Messori, L.; Marcon, G.; Cinellu, M. A.; Bragadin, M.; Folda, A.; Scutari, G.; Bindoli, A. Gold complexes inhibit mitochondrial thioredoxin reductase: consequences on mitochondrial functions. *J. Inorg. Biochem.* **2004**, *98* (10), 1634-1641. DOI: 10.1016/j.jinorgbio.2004.04.020.
(11) Deponte, M.; Urig, S.; Arscott, L. D.; Wolf, K. F.; Reau, R.; Herold-Mende, C.; Koncarevic, S.; Meyer, M.; Davioud-Charvet, E.; Ballou, D. P.; et al. Mechanistic studies on a novel, highly potent gold-phosphole inhibitor of human glutathione reductase. *Journal of Biological Chemistry* **2005**, *280* (21), 20628-20637. DOI: 10.1074/jbc.M412519200.
(12) Serratrice, M.; Cinellu, M. A.; Maiore, L.; Pilo, M.; Zucca, A.; Gabbiani, C.; Guerri, A.; Landini, I.; Nobili, S.; Mini, E.; et al. Synthesis, Structural Characterization, Solution Behavior, and in Vitro Antiproliferative Properties of a Series of Gold Complexes with 2-(2′-Pyridyl)benzimidazole as Ligand: Comparisons of Gold(III) versus Gold(I) and Mononuclear versus Binuclear Derivatives. *Inorg. Chem.* **2012**, *51*, 3161-3171.
(13) Maiore, L.; Cinellu, M. A.; Nobili, S.; Landini, I.; Mini, E.; Gabbiani, C.; Messori, L. Gold(III) complexes with 2-substituted pyridines as experimental anticancer agents: Solution behavior, reactions with model proteins, antiproliferative properties. *J. Inorg. Biochem.* **2012**, *108*, 123-127.
(14) Cai, W.; Zhang, L.; Song, Y.; Wang, B.; Zhang, B.; Cui, X.; Hu, G.; Liu, Y.; Wu, J.; Fang, J. Small molecule inhibitors of mammalian thioredoxin reductase. *Free Radical Biology & Medicine* **2012**, *52*, 257–265.
(15) Gandin, V.; Fernandes, A. P.; Rigobello, M. P.; Dani, B.; Sorrentino, F.; Tisato, F.; Bjornstedt, M.; Bindoli, A.; Sturaro, A.; Rella, R.; et al. Cancer cell death induced by phosphine gold(I) compounds targeting thioredoxin reductase. *Biochemical Pharmacology* **2010**, *79* (2), 90-101. DOI: 10.1016/j.bcp.2009.07.023.
(16) Hickey, J. L.; Ruhayel, R. A.; Barnard, P. J.; Baker, M. V.; Berners-Price, S. J.; Filipovska, A. Mitochondria-targeted chemotherapeutics: The rational design of gold(I) N-heterocyclic carbene complexes that are selectively toxic to cancer cells and target protein

selenols in preference to thiols. *J. Am. Chem. Soc.* **2008**, *130* (38), 12570-+. DOI: 10.1021/ja804027j.
(17) Siciliano, T. J.; Deblock , M. C.; Hindi, K. M.; Durmus, S.; Panzner, M. J.; Tessier, C. A.; Youngs, W. J. Synthesis and anticancer properties of gold(I) and silver(I) N-heterocyclic carbene complexes. *J. Organomet. Chem.* **2011**, *696*, 1066e1071.
(18) Curran, D.; Muller-Bunz, H.; Bar, S. I.; Schobert, R.; Zhu, X. M.; Tacke, M. Novel Anticancer NHC*-Gold(I) Complexes Inspired by Lepidiline A. *Molecules* **2020**, *25* (15). DOI: 10.3390/molecules25153474.
(19) Sulaiman, A. A. A.; Ahmad, S.; Hashimi, S. M.; Alqosaibi, A. I.; Peedikakkal, A. M. P.; Alhoshani, A.; Alsaleh, N. B.; Isab, A. A. Novel dinuclear gold(I) complexes containing bis(diphenylphosphano)alkanes and (biphenyl-2-yl)(di-tert-butyl)phosphane: synthesis, structural characterization and anticancer activity. *New Journal of Chemistry* **2022**, *46* (35), 16821-16831. DOI: 10.1039/d2nj01680j.
(20) Abogosh, A. K.; Alghanem, M. K.; Ahmad, S.; Al-Asmari, A.; Sobeai, H. M. A.; Sulaiman, A. A. A.; Fettouhi, M.; Popoola, S. A.; Alhoshani, A.; Isab, A. A. A novel cyclic dinuclear gold(I) complex induces anticancer activity via an oxidative stress-mediated intrinsic apoptotic pathway in MDA-MB-231 cancer cells. *Dalton Transactions* **2022**, *51* (7), 2760-2769. DOI: 10.1039/d1dt03546k.
(21) Abas, E.; Pena-Martinez, R.; Aguirre-Ramírez, D.; Rodriguez-Dieguez, A.; Laguna, M.; Gras, L. New selective thiolate gold(I) complexes inhibitthe proliferation of different human cancer cellsand induce apoptosis in primary cultures of mousecolon tumors. *Dalton Trans.,* **2020**, *49*, 1915–1927
(22) Filho, M. S.; Scattolin, T.; Dao, P.; Tzouras, N. V.; Benhida, R.; Saab, M.; Van Hecke, C.; Lippmann, P.; Martin, A. R.; Ott, I.; et al. Straightforward synthetic route to gold(I)-thiolato glycoconjugate complexes bearing NHC ligands (NHC = N-heterocyclic carbene) and their promising anticancer activity. *New J. Chem.* **2021**, *45*, 9995-10001.
(23) Rickard, G. A.; Berges, J.; Houee-Levin, C.; Rauk, A. Ab Initio and QM/MM Study of Electron Addition on the Disulfide Bond in Thioredoxin. *J. Phys. Chem. B* **2008**, *112*, 5774-5787.
(24) Howell, J. A. S. DFT investigation of the interaction between gold(I) complexes and the active site of thioredoxin reductase. *Journal of Organometallic Chemistry* **2009**, *694* (6), 868-873. DOI: 10.1016/j.jorganchem.2008.10.029.
(25) Delgado, G. Y. S.; Paschoal, D.; Dos Santos, H. F. Predicting standard reduction potential for anticancer Au(III)-complexes: A DFT study. *Computational and Theoretical Chemistry* **2017**, *1108*, 86-92. DOI: 10.1016/j.comptc.2017.03.027.
(26) Tolbatov, I.; Umari, P.; Marrone, A. Mechanism of Action of Antitumor Au(I) N-Heterocyclic Carbene Complexes: A Computational Insight on the Targeting of TrxR Selenocysteine. *Int. J. Mol. Sci.,,* **2024**, *25*, 2625-2635. DOI: https://doi.org/10.3390/ijms25052625.
(27) Becke, A. D. Density Functional thermochemistry. III. The role of exact exchange. *J. Phys. Chem.* **1993**, *98*, 5648-5652.
(28) Lee, C.; Yang, W.; Parr, R. G. Development of the Cole-Salvetti correlation energy formula into a functional of the electron density. *Phys. Rev. B* **1988**, *37*, 785-789.
(29) Stephens, P. J.; Devlin, F. J.; Chabalowski, C. F.; Frisch, M. J. Ab initio calculations of vibrational absorption and circular-dichroism spectra using density-functional force-fields. *J. Phys. Chem.* **1994**, *98* (45), 11623-11627, Letter. DOI: 10.1021/j100096a001.
(30) Vosko, S. H.; Wilk, L.; Nusair, M. Accurate spin-dependent electron liquid correlation energies for local spin-density calculations - a critical analysis. *Canad. J. Phys.* **1980**, *58* (8), 1200-1211, Article.

(31) Burda, J. V.; Zeizinger, M.; Sponer, J.; Leszczynski, J. Hydration of cis- and trans-platin. A pseudopotential treatment in the frame of a G3-type theory for platinum complexes. *J. Chem. Phys.* **2000**, *113* (6), 2224-2232.
(32) Zeizinger, M.; Burda, J. V.; Šponer, J.; Kapsa, V.; Leszczynski, J. A Systematic ab Initio Study of the Hydration of Selected Palladium Square-Planar Complexes. A Comparison with Platinum Analogues. *J. Phys. Chem. A,* **2001**, *105* (34), 8086-8092.
(33) Zimmermann, T.; Zeizinger, M.; Burda, J. V. Cisplatin Interaction with Cysteine and Methionine; theoretical DFT study. *J. Inorg. Biochem.* **2005**, *99*, 2184-2196.
(34) Zimmermann, T.; Chval, Z.; Burda, J. V. Cisplatin Interaction with Cysteine and Methionine in Aqueous Solution: Computational DFT/PCM Study. *J. Phys. Chem. B* **2009**, *113* (10), 3139-3150. DOI: 10.1021/jp807645x.
(35) Klamt, A.; Schuurmann, G. Cosmo - a New Approach to Dielectric Screening in Solvents with Explicit Expressions for the Screening Energy and Its Gradient. *J Chem. Soc.-Perkin Transactions 2* **1993**, (5), 799-805.
(36) Wertz, D. H. Relationship between the Gas-Phase Entropies of Molecules and Their Entropies of Solvation in Water and 1-Octanol. . *J. Am.chem. Soc.* **1980**, *102*, 5316-5322.
(37) Cheng, M.-J.; Nielsen, R. J.; Goddard III, W. A. *Chem. Commun.* **2014**, *50*, 10994.
(38) Šebesta, F.; Burda, J. V. Side Reactions with an Equilibrium Constraint: Detailed Mechanism of the Substitution Reaction of Tetraplatin with dGMP as a Starting Step of the Pt(IV) Reduction Process. *J. Phys. Chem. B* **2017**, *121*, 4400−4413.
(39) Šebesta, F.; Burda, J. V. Interactions of Ascorbic Acid with Satraplatin and Its Trans Analog JM576; DFT Computational Study. *Eur. J. Inorg. Chem.* **2018**, *13*, 1481–1491. DOI: 10.1002/ejic.201701334.
(40) Zimmermann, T.; Burda, J. V. Charge-scaled cavities in polarizable continuum model: Determination of acid dissociation constants for platinum-amino acid complexes. *J. Chem. Phys.* **2009**, *131*, 135101.
(41) Zimmermann, T.; Burda, J. V. Reaction of cisplatin with cysteine and methionine at constant pH. *Dalton Trans.* **2010**, *39*, 1295-1301.
(42) Zimmermann, T.; Leszczynski, J.; Burda, J. V. Activation of the cisplatin and transplatin complexes in solution with constant pH and concentration of chloride anions; quantum chemical study. *J. Mol. Model.* **2011**, *17*, 2385-2393.
(43) Šebesta, F. S., Ž ; Burda, J.V. Determination of Amino Acids' pKa: Importance of Cavity Scaling within Implicit Solvation Models and Choice of DFT Functionals. *J. Phys. Chem. B* **2024**, *128*, 1627-1616-1637. DOI: https://doi.org/10.1021/acs.jpcb.3c07007.
(44) Reed, A. E.; Weinstock, R. B.; Weinhold, F. Natural population analysis. *J. Chem. Phys.* **1985**, *83* (2), 735-746.
(45) *NBO v 5.9 Program* University of Wisconsin, Madison, Wisconsin 53706: Wisconsin, 2001. www.chem.wisc.edu/~nbo5 (accessed.
(46) Schüürmann, G.; Cossi, M.; Barone, V.; Tomasi, J. Prediction of the p K a of carboxylic acids using the ab initio continuum-solvation model PCM-UAHF. *J. Phys. Chem. A* **1998**, *102* (33), 6706-6712.
(47) Barone, V.; Cossi, M.; Tomasi, J. A new definition of cavities for the computation of solvation free energies by the polarizable continuum model. *J. Chem. Phys.* **1997**, *107* (8), 3210-3221.
(48) Curutchet, C.; Bidon-Chanal, A.; Soteras, I.; Orozco, M.; Luque, F. J. MST Continuum Study of the Hydration Free Energies of Monovalent Ionic Species. *J. Phys. Chem. B* **2005**, *109* (8), 3565-3574.
(49) Orozco, M.; Luque, F. J. Optimization of the cavity size for ab initio MST-SCRF calculations of monovalent ions. . *Chem. Phys.* **1994**, *182*, 237-248.

(50) Zimmermann, T.; Šebesta, F.; Burda, J. B. A new grand-canonical potential for the thermodynamic description of the reactions in solutions with constant pH. *J. Mol. Liquids* **2021**, *335* 115979.
(51) Dunning Jr, T. H. Gaussian basis sets for use in correlated molecular calculations. I. The atoms boron through neon and hydrogen. *J. Chem. Phys.* **1989**, *90* (2), 1007-1023.
(52) Kendall, R. A.; Dunning, T. H.; Harrison, R. J. Electron-Affinities Of The 1st-Row Atoms Revisited - Systematic Basis-Sets And Wave-Functions. *J. Chem. Phys.* **1992**, *96* (9), 6796-6806, Article. DOI: 10.1063/1.462569.
(53) Woon, D. E.; Dunning, T. H. Gaussian-basis sets for use incorrelated molecular calculations.3. The atoms Aluminium through Argon. *J. Chem. Phys.* **1993**, *98* (2), 1358-1371, Article. DOI: 10.1063/1.464303.
(54) Peterson, K. A.; Figgen, D.; Dolg, M.; Stoll, H. Energy-consistent relativistic pseudopotentials and correlation consistent basis sets for the 4d elements Y-Pd. *J. Chem. Phys.* **2007**, *126*, 124101. DOI: 10.1063/1.2647019.
(55) Peterson, K. A.; Puzzarini, C. Systematically convergent basis sets for transition metals. II. Pseudopotential-based correlation consistent basis sets for the group 11 (Cu, Ag, Au) and 12 (Zn, Cd, Hg) elements. *Theor. Chem. Acc.* **2005**, *114*, 283-296 DOI: 10.1007/s00214-005-0681-9.
(56) Figgen, D.; Rauhut, G.; Dolg, M.; Stoll, H. Energy-consistent pseudopotentials for group 11 and 12 atoms: adjustment to multi-configuration Dirac-Hartree-Fock data. *J. Chem. Phys.* **2005**, *311*, 227-244. DOI: 10.1016/j.chemphys.2004.10.005.
(57) Pritchard, B. P.; Altarawy, D.; Didier, B.; Gibson, T. D.; Windus, T. L. A New Basis Set Exchange: An Open, Up-to-date Resource for the Molecular Sciences Community. *J. Chem. Inf. Model.* **2019**, *59*, 4814-4820.
(58) Feller, D. The role of databases in support of computational chemistry calculations. *J. Comput. Chem.* **1996**, *17*, 1571-1586.
(59) Schuchardt, K. L.; Didier, B. T.; Elsethagen, T.; Sun, L.; Gurumoorthi, V.; Chase, J.; Li, J.; Windus, T. L. Basis Set Exchange: A Community Database for Computational Sciences. *J. Chem. Inf. Model.* **2007**, *47*, 1045-1052. DOI: 10.1021/ci600510j.
(60) Urban, M.; Černušák, I.; Kello, V.; Noga, J. Electron Correlation in Molecules. In *Methods in Computational Chem.*, Wilson, S. Ed.; Vol. 1; Plenum Press, 1987.
(61) Jurecka, P.; Hobza, P. On the convergence of the (dE(CCSD(T))-dE(MP2)) term for complexes with multiple H-bonds. *Chem. Phys. Lett.* **2002**, *365* (1), 89-94.
(62) Bryantsev, V. S.; Diallo, M. S.; Goddard Iii, W. A. Calculation of Solvation Free Energies of Charged Solutes Using Mixed Cluster/Continuum Models. *J. Phys. Chem. B* **2008**, *112* (32), 9709-9719. DOI: 10.1021/jp802665d.
(63) Gupta, M.; da Silva, E. F.; Svendsen, H. F. Explicit Solvation Shell Model and Continuum Solvation Models for Solvation Energy and p K a Determination of Amino Acids. *J. Chem. Theor. Comput.* **2013**, *9* (11), 5021-5037.
(64) Casasnovas, R.; Fernández, D.; Ortega-Castro, J.; Frau, J.; Donoso, J.; Muñoz, F. Avoiding gas-phase calculations in theoretical pK a predictions. *Theor. Chem. Acc.* **2011**, *130* (1), 1-13.
(65) Sastre, S.; Casasnovas, R.; Muñoz, F.; Frau, J. Isodesmic reaction for accurate theoretical p K a calculations of amino acids and peptides. *Phys. Chem. Chem. Phys.* **2016**, *18* (16), 11202-11212.
(66) Lide, D. R. CRC Handbook of Chemistry and Physics; 7-1 Properties of Amino Acids. 88th ed.; CRC Press: 2007; Vol. 7-1 Properties of Amino Acids, p 2640.
(67) Huber, R. E.; Criddle, R. S. Comparison of the Chemical Properties of Selenocysteine and Selenocystine with Their Sulfur Analogs. *Arch. Biochem. Biophys.* **1967**, *122*, 164-173.

(68) Burda, J. V.; Futera, Z.; Chval, Z. Exploration of various electronic properties along the reaction coordinate for hydration of Pt(II) and Ru(II) complexes; the CCSD, MPx, and DFT computational study. *J. Mol. Model.* **2013**, *19* (12), 5245-5255. DOI: 10.1007/s00894-013-1994-6.
(69) Murdoch, J. R. What is the rate-limiting step of a multistep reaction? *Journal of Chemical Education* **1981**, *58* (1), 32. DOI: 10.1021/ed058p32.
(70) Alberty, R. A. Effect of Ph and Metal Ion Concentration on Equilibrium Hydrolysis of Adenosine Triphosphate to Adenosine Diphosphate. *Journal of Biological Chemistry* **1968**, *243* (7), 1337-&.
(71) Alberty, R. A.; Oppenheim, I. Fundamental equation for systems in chemical equilibrium. *The J. Chem. Phys.* **1988**, *89* (6), 3689-3693.
(72) Alberty, R. A. Biochemical thermodynamics *Biochem Biophys Acta* **1994**, *1207*, 1–11
(73) Alberty, R. A. Use of Legendre transforms in chemical thermodynamics - (IUPAC Technical Report). *Pure and Applied Chemistry* **2001**, *73* (8), 1349-1380.
(74) Šebesta, F.; Šebera, J.; Sychrovský, V.; Tanaka, Y.; Burda, J. V. QM and QM/MM umbrella sampling MD study of the formation of Hg(II)–thymine bond: Model for evaluation of the reaction energy profiles in solutions with constant pH. *J. Comput. Chem.* **2020**, *41*, 1509–1520.
(75) Michera, L.; Nekardova, M.; Burda, J. V. Reactions of cisplatin and glycine in solution with constant pH: a computational study. *Phys. Chem. Chem. Phys.* **2012**, *14*, 12571-12579.

View Article Online
DOI: 10.1039/D4CP04386C

Table 1 pKa values from selected levels of calculations including the nuclear degrees of freedom using Wertz correction. Plot of calculated vs. experimental values together with fits for all the used method is in SI – part 1.

	DP_B3/D	DP_M06/D	DP/T	MP2/D	CC/D	MP2/T	CCe/T	Exp.[66, 67]
Cys(COO)[a)]	3.5	**2.8**	4.3	0.7	1.7	3.0	4.0	1.9
Cys(S)	11.5	**8.3**	11.7	11.6	12.9	12.6	13.8	8.3
Cys(NH_2)	15.8	**13.5**	15.7	16.1	15.9	15.4	15.3	10.7
Sec(COO)	3.0	**2.4**	3.6	0.7	1.7	2.7	3.8	1.9
Sec(Se)	8.0	**6.4**	8.3	7.4	8.9	9.2	10.6	5.7
Sec(NH_2)	14.4	**13.3**	15.1	16.0	15.9	15.3	15.2	10.0
Au-NHC	18.6	**16.1**	18.0	15.9	17.6	16.0	17.8	
Au-NHC-Cys(S)	0.1	**-2.9**	0.8	-2.1	-0.5	-1.6	0.0	
Au-NHC-Cys(COO)	2.3	**1.2**	2.2	-0.8	0.1	1.5	2.4	
Au-NHC-Cys(NH_2)	8.7	**5.8**	9.1	8.0	7.9	7.5	7.5	
Au-$(NHC)^-$-Cys[b)]	26.4	**23.5**	17.6	23.9	25.5	24.2	25.8	
Au-NHC-Sec(Se)	-6.4	**-9.6**	-2.3	-9.6	-7.5	-8.9	-6.8	
Au-NHC-Sec(COO)	2.4	**-0.9**	2.4	-0.1	0.8	2.0	2.9	
Au-NHC-Sec(NH_2)	12.1	**9.4**	11.6	11.5	11.5	11.0	11.0	
Au-$(NHC)^-$-Sec[b)]	21.8	**19.5**	16.2	19.5	21.1	20.2	21.8	
HCl	-7.6	**-10.1**	-6.1	-7.9	-6.3	-0.2	-0.6	-7.0
K_w	16.0	**16.9**	16.8	13.6	15.4	16.9	17.7	14.0
RMSD	2.9	2.2	3.3	3.2	3.5	4.1	4.5	

[a)] Cys(COO) means deprotonation of carboxyl group, Cys(S) subsequent deprotonation of thiol group, and Cys(NH_2) third deprotonation on NH_2 group (e.g., anion with charge -2e). And in analogy all remaining system with amino acids.

[b)] (fourth) deprotonatation on imidazole ring, $(NHC)^-$.

Table 2 Gibbs free energies for stationary structures from individual reaction coordinates (in kcal/mol), the reactant supermolecules is taken as a zero-reference level; R means reactants, P products, I intermediate, TS transition state (single-step without any number, 1 and 2 distinguish those points in two steps mechanism).

	Opt/D	DP_B3/D	DP_M06/D	CP/T	Opt/T	DP/T	CP/Q	MP2/D	CC/D	MP2/T	CCe/T	CC/T
Cysteine												
R	0.0	0.0	0.0	0.0	0.0	0.0	0.0	0.0	0.0	0.0	**0.0**	0.0
TS	6.9	11.6	10.4	8.1	8.1	12.0	8.4	12.9	12.2	13.8	**13.2**	13.1
P	-15.2	-13.3	-13.4	-13.4	-13.6	-14.5	-13.9	-13.8	-13.0	-13.8	**-13.2**	-13.0
R	0.0	0.0	0.0	0.0	0.0	0.0	0.0	0.0	0.0	0.0	**0.0**	
TS1	10.5	12.3	13.9	8.5	9.2	8.8	10.0	14.4	16.2	10.4	**12.1**	
I	10.2	11.7	10.3	7.6	6.6	7.5	9.2	13.6	13.7	9.6	**10.5**	
TS2	22.2	15.5	12.5	17.7	19.4	11.9	19.5	19.2	18.9	16.0	**15.5**	
TS	11.8	9.4	9.8	11.8	12.1	8.4	12.5	9.6	9.9	8.5	**8.0**	
P	-2.2	-6.8	-6.3	-4.0	-4.6	-8.4	-4.8	-4.9	-3.2	-7.1	**-5.4**	
	Selenocysteine											
R	0.0	0.0	0.0	0.0	0.0	0.0	0.0	0.0	0.0	0.0	**0.0**	0.0
TS	6.5	11.0	8.7	7.9	7.1	11.1	7.4	9.4	8.2	10.8	**10.5**	10.2
P	-14.7	-15.6	-14.0	-14.6	-14.8	-15.7	-14.7	-14.5	-13.6	-14.6	**-13.7**	-13.8
R	0.0	0.0	0.0	0.0	0.0	0.0	0.0	0.0	0.0	0.0	**0.0**	
TS1	11.4	9.5	12.5	11.1	10.5	10.9	10.1	14.1	16.0	11.9	**13.7**	
I	8.0	6.2	6.7	7.2	5.5	7.4	5.9	10.5	10.7	9.0	**10.0**	
TS2	19.5	10.5	13.6	17.0	17.7	10.8	16.3	15.1	15.0	13.4	**13.3**	
TS_	10.1	8.3	11.2	11.9	9.0	7.5	9.6	7.6	7.6	7.4	**7.4**	
P	-6.4	-11.6	-10.4	-6.8	-7.8	-10.5	-8.9	-8.9	-7.2	-10.8	**-9.1**	
RMSD	3.7	2.3	2.0	3.1	3.3	2.3	3.0	1.6	2.2	1.1		0.2

Table 3 Rate constants of the formation of Au(I)-NHC complex with Cys or Sec; rate constants k_1, and k_2 correspond with forward reactions and k_{-1}, and k_{-2} with reverse reactions in the two-step mechanism, k_{tot} means the overall rate constant for this mechanism obtained according to (eq 6).

	Opt/D	DP_B3/D	DP_M06/D	CP/T	Opt/T	DP_B3/T	CP/Q	MP2/D	CC/D	MP2/T	CCe/T
Deprotonated *branch –* ***one-step*** *mechanism*											
k(Cys)	5.1E+07	2.1E+04	1.5E+05	7.6E+06	7.1E+06	9.6E+03	4.4E+06	2.1E+03	6.9E+03	4.9E+02	1.6E+03
k(Sec)	1.0E+08	5.0E+04	2.7E+06	9.2E+06	4.0E+07	3.3E+05	2.3E+07	8.1E+05	6.5E+06	7.8E+04	2.0E+05
Protonated *branch –* ***one-step*** *mechanism*											
k(Cys)	1.4E+04	8.3E+05	1.5E+04	8.0E+04	7.9E+03	4.5E+06	3.9E+03	5.7E+05	3.4E+05	3.8E+06	8.9E+06
k(Sec)	2.6E+05	4.7E+06	3.6E+04	1.2E+04	1.4E+06	2.1E+07	6.0E+05	1.6E+07	1.6E+07	2.5E+07	2.4E+07
Protonated *branch –* ***two-step*** *mechanism*											
k_1(Cys)	1.2E+05	6.1E+03	4.0E+02	3.5E+06	1.1E+06	2.1E+06	2.7E+05	1.7E+02	7.6E+00	1.4E+05	8.2E+03
k_{-1}(Cys)	3.5E+12	2.4E+12	1.5E+10	1.2E+12	7.2E+10	7.1E+11	1.5E+12	1.7E+12	8.8E+10	1.6E+12	4.1E+11
k_2(Cys)	9.7E+03	1.0E+10	1.6E+11	2.2E+05	2.3E+03	4.0E+09	1.8E+05	1.9E+09	7.2E+10	1.3E+08	1.3E+09
k_{-2}(Cys)	7.4E-06	3.7E+03	1.1E-01	6.6E-04	1.6E-05	7.6E-03	6.2E-07	1.4E-05	4.1E-04	1.2E-02	2.9E-03
k_{tot}(Cys)	3.3E-04	2.6E+01	3.7E+02	6.1E-01	3.6E-02	1.2E+04	3.2E-02	1.9E-01	3.5E+00	1.2E+01	2.5E+01
k_1(Sec)	2.6E+04	6.4E+05	4.1E+03	4.5E+04	1.3E+05	6.4E+04	2.2E+05	2.7E+02	1.1E+01	1.2E+04	5.2E+02
k_{-1}(Sec)	1.8E+10	2.1E+10	3.4E+08	8.5E+09	1.0E+09	1.8E+10	4.4E+09	1.4E+10	7.8E+08	4.4E+10	1.1E+10
k_2(Sec)	2.3E+04	4.0E+09	5.8E+07	3.7E+05	6.8E+03	2.3E+10	1.2E+17	3.0E+09	4.7E+09	3.6E+09	2.3E+10
k_{-2}(Sec)	7.2E-07	4.9E+01	1.6E-05	1.8E-05	3.2E-07	1.6E-03	2.1E-06	1.6E-05	3.3E-04	1.1E-05	2.4E-04
k_{tot}(Sec)	3.3E-02	1.0E+05	6.1E+02	1.9E+00	9.1E-01	3.6E+04	2.2E+05	4.7E+01	9.2E+00	8.8E+02	3.5E+02

View Article Online
DOI: 10.1039/D4CP04386C

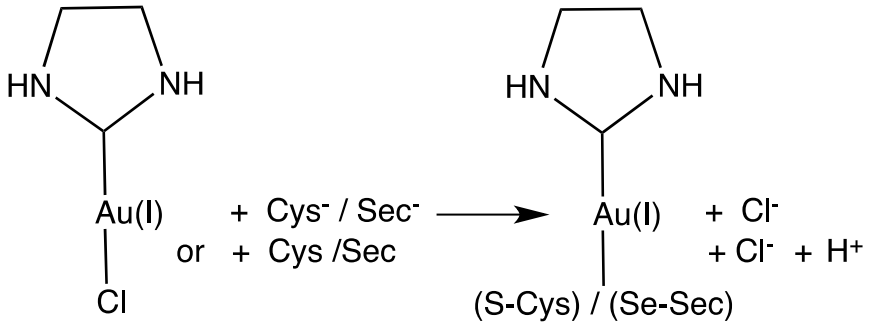

Scheme 1 Coordination reaction of gold(I) complex with Cys/Sec amino acid

View Article Online
DOI: 10.1039/D4CP04386C

Captions to Figures

Figure 1. Reaction energy profile for coordination of the Au(I)-NHC model complex to Cys (blue lines) and Sec (red lines). Solid lines label reactions in deprotonated forms, dashed lines in protonated forms (for simulation of (more) acidic solutions). The upper structures display stationary points of the two-step reaction mechanism for interaction of gold complex with selenocysteine, the lower structures interaction with deprotonated cysteine amino acid.

Figure 2. Proton chemical potential of selected neutral molecules occurring on the reaction coordinate.

Figure 3. Dependence of the reaction Gibbs-Alberty free energy (in kcal/mol) on pH of solution. Coordination energy of Cys - black dashed line, Sec – red solid line.

View Article Online
DOI: 10.1039/D4CP04386C

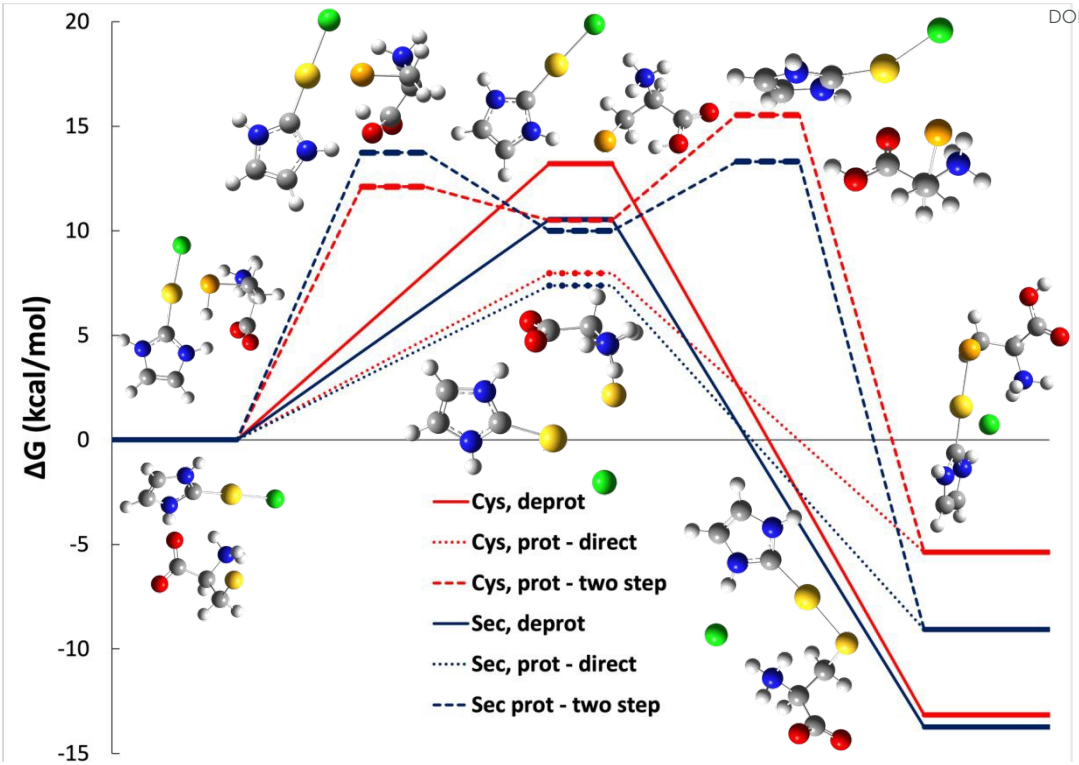

Figure 1

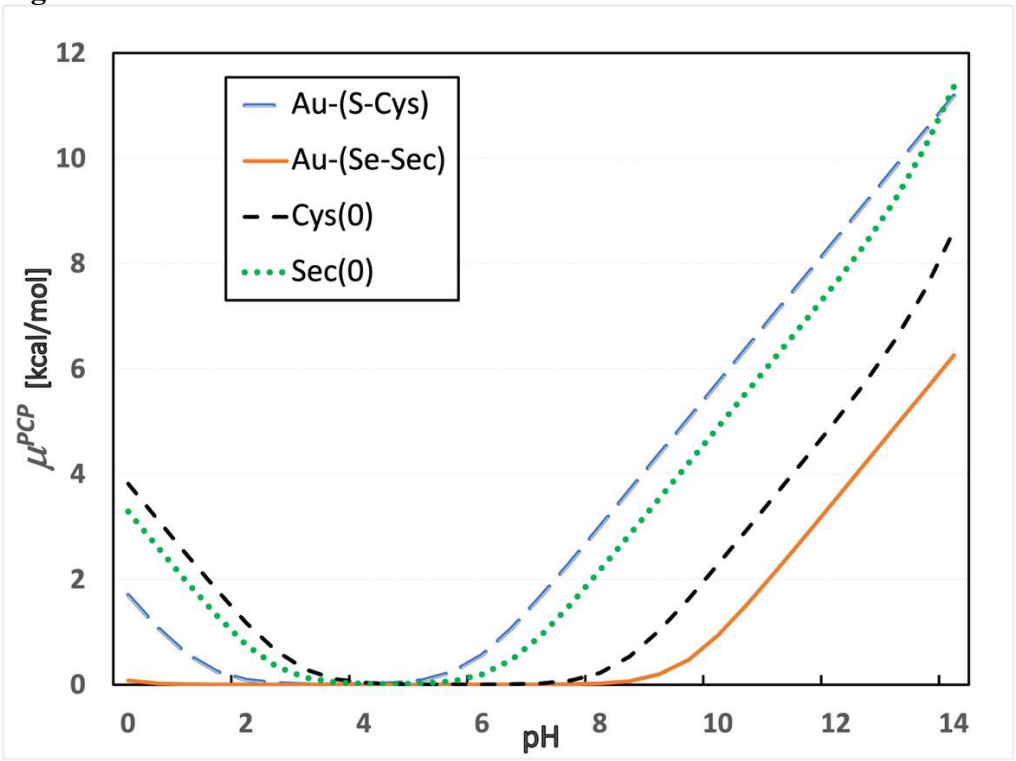

Figure 2

View Article Online
DOI: 10.1039/D4CP04386C

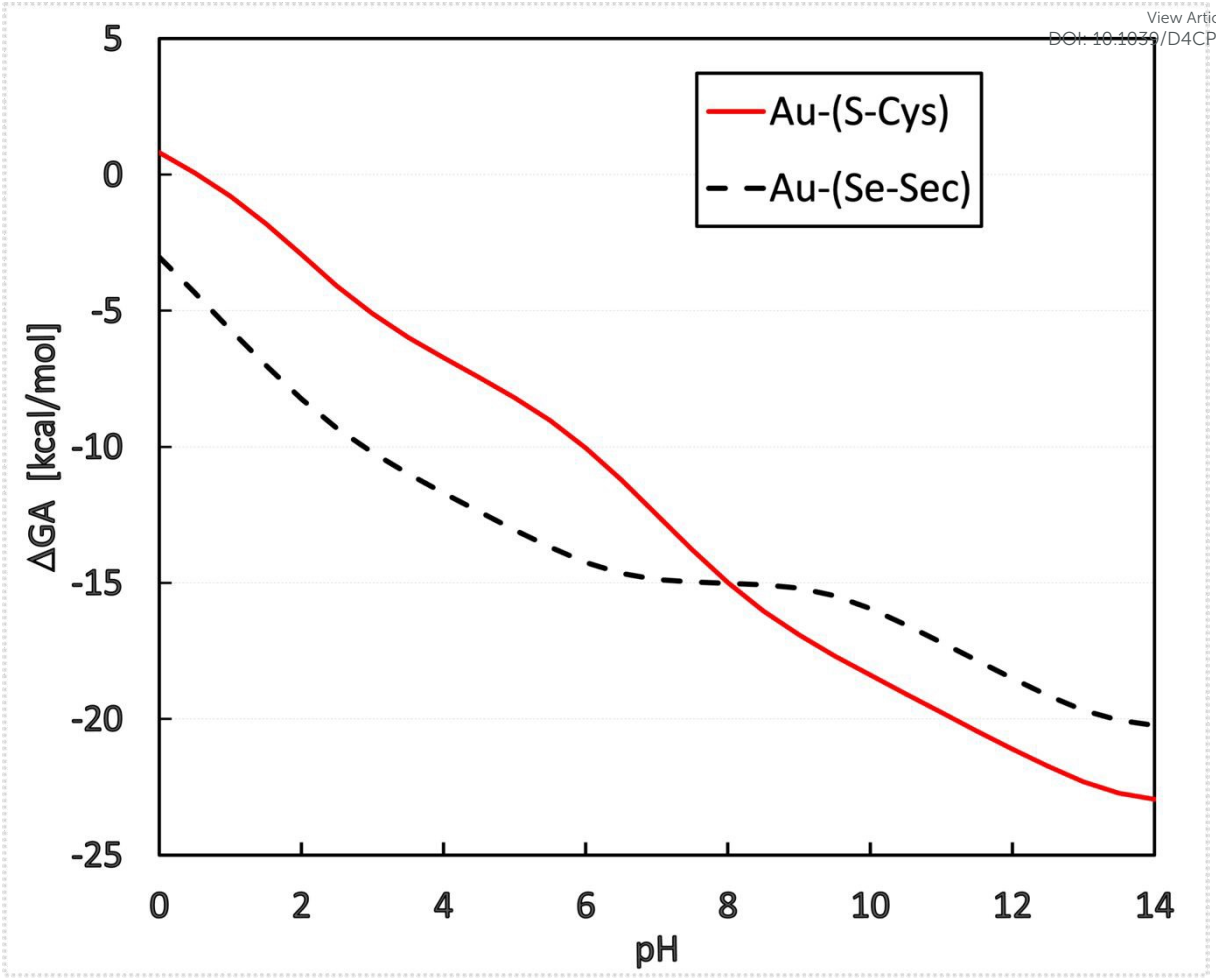

Figure 3

View Article Online
DOI: 10.1039/D4CP04386C

All necessary data are present in the form of Tables and Figures. Supplementary Information is provided for the optimized basis sets by authors. Programs used within the study are clearly specified and openly available.
Additional information can be obtained upon request using the address of corresponding author.